REVIEW

Silicon nanoparticles: fabrication, characterization, application and perspectives

Taeyeong Kim[1] and Jungchul Lee[1*]

Abstract

Silicon nanoparticles have emerged as pivotal components in nanoscience and nanoengineering due to their inherent characteristics such as high energy capacity and outstanding optical properties. Numerous fabrication and characterization techniques have been researched so far, while a range of applications utilizing them have been developed. In this review, we aim to provide a brief overview of the distinct and representative fabrication methods of silicon nanoparticles, including top-down, bottom-up, and reduction approaches. Then, we look into various characterization techniques essential for assessing and ensuring quality and performance of fabricated silicon nanoparticles. In addition, we provide insights for silicon nanoparticle technology towards further advancements.

Introduction

Silicon stands as the second most abundant element on earth, surpassed only by oxygen. Its ample presence and cost-effectiveness has made it one of the most accessible inorganic materials available. Over the past few decades, the global semiconductor-related industries have experienced rapid growth, underlining the significant role of silicon. One mainstream application of silicon in recent technological advancements has been in the realm of energy storage. Compared to graphite, silicon boasts a specific capacity that is more than 10 times greater (4200 mAh/g as opposed to 372 mAh/g) [1]. This makes it a prime candidate for high-capacity battery anode materials. Further studies have shown that when silicon particles are sized below 150 nm, they can mitigate the cracking issues experienced during the repeated lithiation and delithiation processes [2]. Another major application lies in the optical domain. Silicon nanoparticles with sizes ranging from 100 to 200 nm can be used for applications that exhibit structural colors due to Mie resonance [3]. When they are scaled down to the order of 1 nm, it emerges as a photonic material, specifically quantum dots. Intriguingly, the confinement effect dictates that the smaller these quantum dots are, the stronger their luminescent properties.

In this review, we aim to overview the fabrication technology of silicon nanoparticles. Then, we look into the characterization method of fabricated silicon nanoparticles and their applications. We also offer perspectives on future directions of silicon nanoparticle technology.

Fabrication

Among the fabrication methods for silicon nanoparticles, the top-down approach stands out in terms of quality attributes such as purity and uniformity. As the name intuitively suggests, the top-down method involves breaking down bulk silicon into nanoparticles. One of the strategies for this is through the electrochemical etching of silicon wafers [11]. For p-type (100) silicon wafers with resistivity ranging from 1–10 Ω-cm, a mixture of HF and H_2O serves as the etchant. This procedure can yield colloidal suspensions of silicon particles around 150 nm in diameter. Silicon nanoparticles can also be mechanically produced through grinding, either by utilizing a mechanical milling process or grinding bulk silicon in a blender (Fig. 1a) [4, 12]. While the distribution of the fabricated particles tends to be broad, stratification by

*Correspondence:
Jungchul Lee
jungchullee@kaist.ac.kr
[1] Department of Mechanical Engineering, Korea Advanced Institute of Science and Technology, 291 Daehak-ro, Daejeon 34141, Republic of Korea
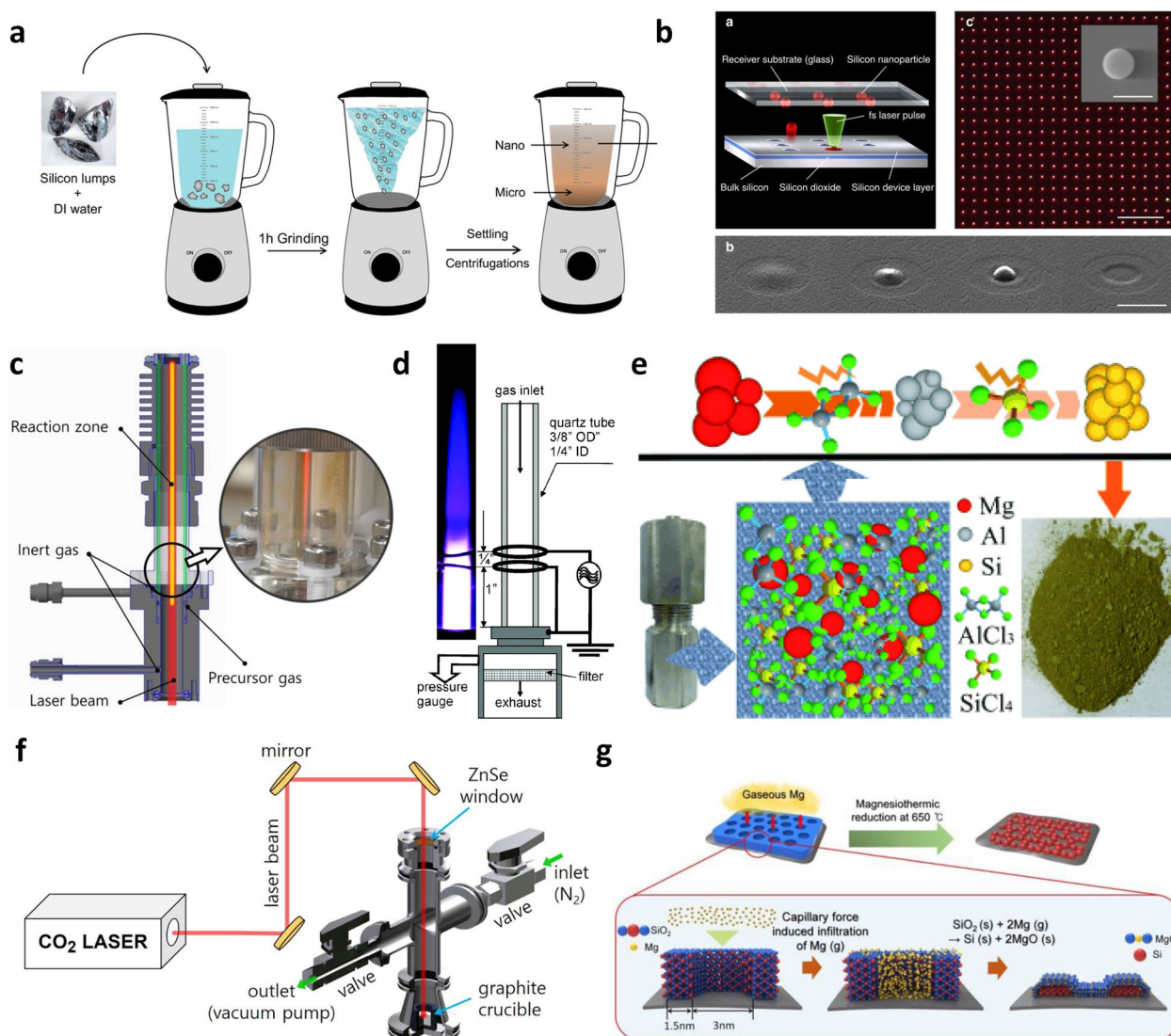
Fig. 1 Various production methods for silicon nanoparticles. **a** Grinding of silicon lumps in liquid (Top-down). Reprinted from [4] with permission from American Chemical Society. **b** Laser printing on to the glass substrate (Top-down). Reprinted from [5] with permission from Springer Nature. **c** Laser pyrolysis of silane (SiH_4) (Bottom-up). Reprinted from [6] with permission from Springer Nature. **d** Plasma pyrolysis of silane (SiH_4) (Bottom-up). Reprinted from [7] with permission from American Chemical Society. **e** Reduction of tetrachlorosilane ($SiCl_4$) (Bottom-up). Reprinted from [8] with permission from John Wiley and Sons. **f** Carbonthermal reduction of silica (Reduction). Reprinted from [9] (CC BY 4.0). **g** Magnesiothermic reduction of silica (Reduction). Reprinted from [10] (CC BY 4.0)

size within the solution allows for its minimization, enabling the production of silicon nanoparticles ranging from 100–400 nm in diameter. These methods have the advantage of a relatively simple production process, but a drawback is the reduced sphericity of the resulting silicon nanoparticles. On the other hand, laser ablation offers a method to produce spherical silicon nanoparticles. Similar to the previous method, it subtracts from bulk silicon, utilizing laser irradiation in a liquid to produce a colloidal solution [13–15]. While nanosecond, picosecond, and femtosecond lasers are employed, shorter pulses have the advantage of minimizing thermal effects and the interaction between laser pulses and cavitation bubbles, thereby producing smaller silicon nanoparticles [16]. The size distribution of the produced nanoparticles tends to be broad, but particles several nm and larger can be manufactured. Beyond colloidal forms, there's also a method involving laser printing onto a substrate. By exposing a silicon wafer to a ring-shaped femtosecond laser intensity, molten silicon nanodroplets can be transferred to a glass surface, allowing for the fabrication of silicon nanoparticles larger than 400 nm in diameter [17].

Alternatively, when a Gaussian laser pulse is applied to the top of an SOI wafer, the device layer undergoes rapid heating and localized melting, facilitating its transfer to the upper glass substrate (Fig. 1b) [5]. This produces silicon nanoparticles with diameters exceeding 160 nm. While there are production volume limitations, a notable advantage is the ability to position high-sphericity silicon nanoparticles precisely where desired on the substrate.

The bottom-up fabrication method for silicon nanoparticles is advantageous in terms of mass production. Initially, silicon nanoparticles can be produced through the pyrolysis of silane (SiH_4), a gaseous precursor, primarily via laser heating or plasma heating. For laser heating, CO_2 lasers are predominantly used because silane has an efficient absorption at 10.6 μm wavelength [18]. By introducing a gas flow and heating it with a laser, silicon nanoparticles can be collected on a collector (Fig. 1c) [6, 19, 20]. Not only lasers, but plasmas can also be used to produce silicon particles (Fig. 1d) [7]. Using this method, silicon nanoparticles primarily larger than 10 nm can be produced in large quantities, but a drawback is the difficulty in controlling the particle size. Silicon nanoparticles can also be produced by reducing the liquid precursor silicon tetrachloride ($SiCl_4$). Initially, silicon nanoparticles were produced under high-temperature and high-pressure conditions using Na as a reducing agent [21]. Subsequently, technologies were developed to produce them at room temperature using NaSi and KSi as reducing agents [22]. Recently, similar methods based on organic solutions have been used to produce silicon nanoparticles (Fig. 1e) [8, 23]. Through this method, silicon nanoparticles larger than 10 nm can be produced at a lower cost compared to using silane. However, they still face challenges in size control and the generation of by-products.

Another method to produce silicon nanoparticles is through the reduction of silica nanoparticles. Due to the strong bond between silicon and oxygen atoms, a significant amount of energy is required to reduce silica to silicon [24]. When silica nanoparticles are heated with carbon at high temperatures, a carbothermal reduction reaction occurs, enabling the production of silicon nanoparticles with diameters ranging from 80 to 200 nm (Fig. 1f) [9, 25]. Additionally, using magnesium as a reducing agent for silica, silicon nanoparticles can be produced through the magnesiothermic reduction reaction (Fig. 1g) [26, 27]. Since this process takes place at temperatures above the melting point of magnesium, which is 650 °C, it can be conducted at temperatures lower than the carbothermal reduction of silica particles, which requires temperatures above 2000 °C [28]. Through this method, it is possible to produce silicon nanoparticles at a scale of 10 nm [10]. However, magnesiothermic reduction for silicon production presents a significant limitation due to inevitable incomplete reduction, resulting in unreacted silica or magnesium silicide formation.

The advantages and challenges of each fabrication method explained previously are summarized in Table 1. In addition, the size range and uniformitiy of silicon nanoparticle produced by different fabrication processes are summarized in Table 2.

The fabricated silicon nanoparticles can have their energy levels finely tuned through a doping process. In the fabrication of silicon nanoparticles using a top-down process, the utilization of doped n-type or p-type silicon as the starting material enables the production of doped silicon nanoparticles [29]. In the bottom-up fabrication of silicon nanoparticles, the introduction of silane along with precursor gases enables the production of doped silicon nanoparticles [30]. The silicon nanoparticles can also be doped post fabrication through solution processing and annealing [31]. For boron doping, a boric acid solution is mixed with silicon nanoparticles and then

Table 1 Advantages and challenges of silicon nanoparticle fabrication method

Method		Advantages	Challenges
Top-down	Etching and grinding	Relatievily simple fabrication process	Reduced sphericity of the resulting silicon nanoparticles
	Laser ablation	Spherical silicon nanoparticles	Broad size distribution
	Laser printing	Spherical silicon nanoparticles positioned at desired location	Production volume limitation
Bottom-up	Pyrolysis of silane	Mass production	Difficulty in controlling the nanoparticle size
	Reduction of silicon tetrachlorid	Mass production with low cost	Difficulty in controlling the nanoparticle size and generation of by-products
Reduction of silica particles	Carbothermal reduction	Reduction of relatively inexpensive silica for silicon nanoparticle production	Reaction at temperatures above 2000 °C
	Magnesiothermic reduction	Reduction of relatively inexpensive silica for silicon nanoparticle production at temperatures around 650 °C	Incomplete reduction resulting in the formation of unreacted silica or magnesium silicide

Table 2 Size range and uniformity of silicon nanoparticle fabrication method

Method		Size range	Uniformity
Top-down	Etching and grinding	100–400 nm	Low
	Laser ablation	Larger than several nm	Low
	Laser printing	160–400 nm	High
Bottom-up	Pyrolysis of silane	Larger than 10 nm	Low
	Reduction of silicon tetrachlorid	Larger than 10 nm	Low
Reduction of silica particles	Carbothermal reduction	80–200 nm	Low
	Magnesiothermic reduction	10–350 nm	Low

dried to form a powder. Upon annealing the powder at 900 °C in an argon environment, doped silicon nanoparticles are obtained.

Characterization

The fabricated silicon nanoparticles are stored either in powder or colloid forms and are characterized based on their shape, size, mass, crystallinity, and other properties (Fig. 2). Typically, for nanoparticles with diameters above 100 nm, Scanning Electron Microscopy (SEM) is used, while for those under 100 nm, Transmission Electron Microscopy (TEM) is the method of choice. While SEM and TEM are widely used to analyze both the shape and size of nanoparticles, the number of nanoparticles that can be analyzed through these imaging techniques is limited. Therefore, to analyze the size distribution of particles, Dynamic light scattering (DLS) is predominantly

used [39, 40]. For mass, it can be calculated using the known size and density of the silicon particles. Assuming a spherical shape, the size and density measured through Small Angle X-ray Scattering (SAXS) or Differential Centrifugal Sedimentation (DCS) can also be used for calculation [41]. Additionally, single nanoparticle mass can be measured using capillary resonators or solid microchannel resonators [42, 43].

Notably, silicon nanoparticles produced via reduction may not be entirely reduced to silicon, and impurities might be present. The elemental composition of the silicon nanoparticle clusters can be quantified using X-ray Photoelectron Spectroscopy (XPS) spectra (Fig. 3a) [32]. The crystallinity of silicon nanoparticles is another essential metric. Amorphous silicon benefits battery anodes, while crystalline silicon is preferable for optical applications [44, 45]. This can be verified through
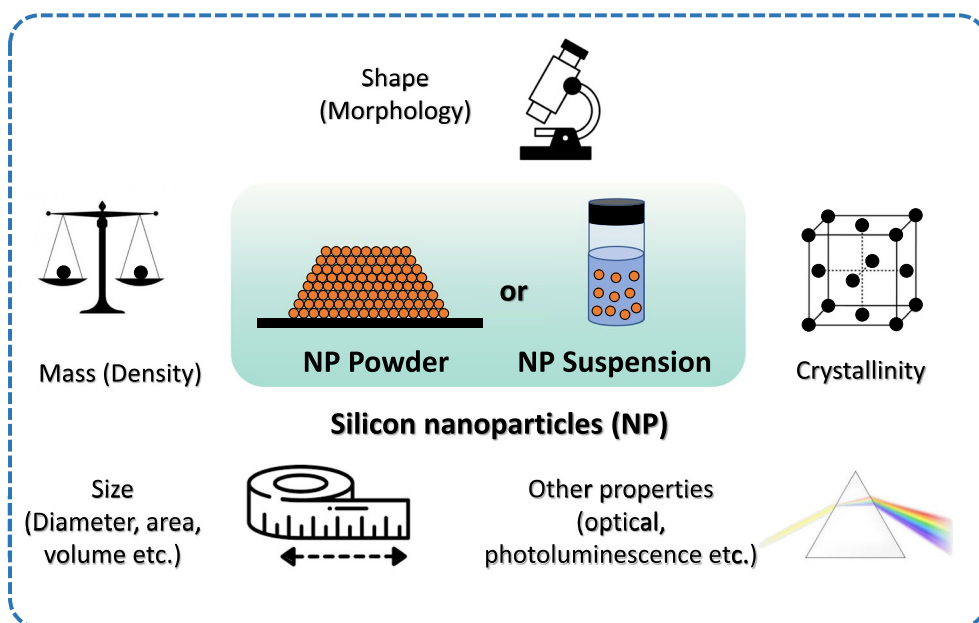

Fig. 2 Characterization of silicon nanoparticles. Size, shape, mass, crystallinity, and other properties of silicon nanoparticles are measured with a variety of equipments considering whether nanoparticles are in powder form or in suspension
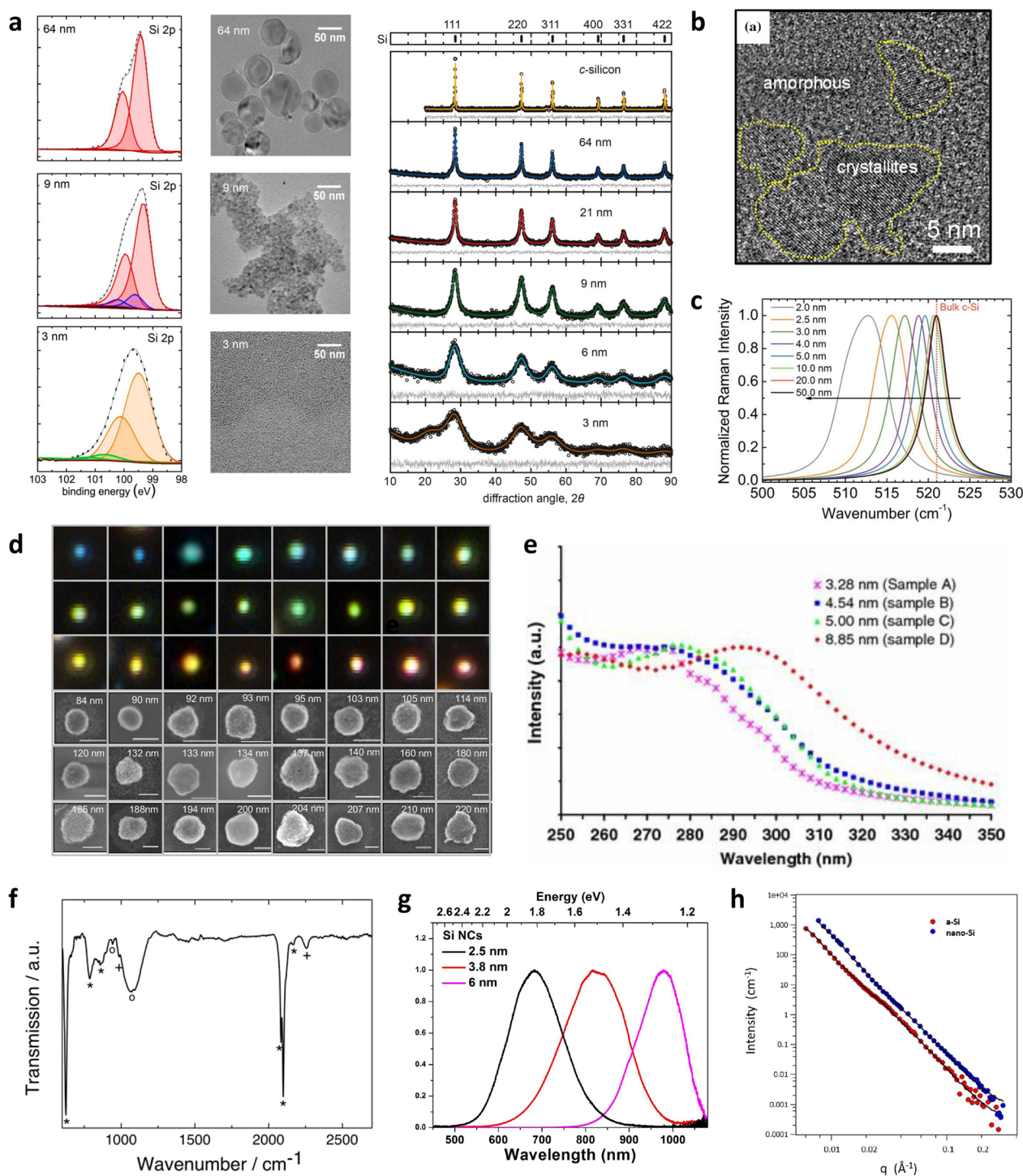
Fig. 3 **a** (left) XPS spectras, (center) Bright-field TEM images, (right) XRD patterns. Reprinted from [32] with permission from American Chemical Society. **b** HRTEM image of a region of milled silicon nanoparticle. Reprinted from [33] with permission from Springer Nature. **c** Calculated Raman spectra of silicon nanocrystals with various sizes. Reprinted from [34] with permission from AIP Publishing. **d** (top) Experimental scattering color visible range of selected silicon nanoparticles and (bottom) their corresponding SEM images for different values of diameters from 84 to 220 nm. Reprinted from [4] with permission from American Chemical Society. **e** UV–Vis spectra of the silicon nanoparticles. Reprinted from [35] with permission from Springer Nature. **f** FT-IR spectrum of silicon nanoparticle powder measured in diffuse reflection. Reprinted from [36] (CC BY 4.0). **g** Photoluminescence spectra of silicon nanocrystals of 2.5, 3.8 and 6.2 nm diameter. Reprinted from [37] (CC BY 4.0). **H** SANS data for a-Si and nano-Si before ball milling with corresponding fits (continuous lines) based on size distributions obtained via a Monte Carlo analysis. Reprinted from [38] (CC BY 4.0)

High-Resolution TEM (HRTEM) imaging, X-ray Diffraction (XRD), and Raman spectroscopy (Fig. 3a–c) [32–34]. XRD not only provides information about crystallinity but also shows that as the diameter of the silicon nanoparticles decreases, the peaks become broader, indicating a change in particle size. Also, Raman spectroscopy not only reveals crystallinity but is also influenced by particle size. As the particle size decreases, a redshift and the broadening of the Full Width at Half Maximum (FWHM) occurs. This phenomenon is due to the size effect of silicon nanoparticles where phonon vibrations are trapped in nanoparticles [46].

Silicon nanoparticles exhibit Mie resonance of electric and magnetic dipoles in the visible light spectrum [47, 48]. To analyze this, single silicon nanoparticles are positioned on a glass substrate, and a dark field image captures the Mie scattering characteristics (Fig. 3d). This property is prominent in silicon nanoparticles with diameters between 100 and 200 nm. Various silicon nanoparticle diameters enable Mie resonators to tune vibrant broad-spectrum colors in a dark background to RGB [4]. Colloids of dispersed silicon nanoparticles can be analyzed using Ultraviolet-Visible (UV–Vis) spectroscopy (Fig. 3e) [35, 49]. The optical properties of silicon nanoparticles, sensitive to factors like size, shape, concentration, aggregation state, and refractive index, can be characterized using UV-Vis, and the colloidal stability can be analyzed. Fourier-Transform Infrared Spectroscopy (FTIR) offers insights into bond strength, characteristics, specific functional group band positions, and molecular structure interactions (Fig. 3f) [36]. When the silicon nanoparticles are reduced to a few nm, the quantum confinement-induced photoluminescence energy can be extensively adjusted (Fig. 3g) [50]. High photoluminescence quantum yields, up to 60%, have been reported for silicon nanoparticle colloids [51]. Efforts to expand the tunability of photoluminescence by adjusting nanoparticle size are ongoing. A blue shift in the PL peak is evident as nanoparticle size decreases due to enhanced quantum confinement [37]. Small Angle Neutron Scattering (SANS) measurements not only offer general information about particle size but, through scattering data analysis, allow estimation of the internal surface area per volume unit of the material (Fig. 3h) [38]. This is especially beneficial for materials with chemically altered surfaces, and it can be utilized for characterizing porous structures.

Application

The primary applications of silicon nanoparticles are in energy, specifically as anode materials for lithium-ion batteries, and in optics as Mie resonators. Silicon, as previously mentioned, has an energy capacity that's over 10 times that of carbon, making it a promising candidate for next-generation anode materials. One of the challenges with silicon is the cracking that occurs during the lithiation and delithiation processes, which can impair performance. However, using silicon nanoparticles smaller than 150 nm can mitigate these cracking issues (Fig. 4a) [2]. Recently, there's been an interest in combining silicon nanoparticles with amorphous carbon, graphene, and carbon nanotubes [57]. Through this approach, numerous electrical contact points are provided, and the pathway for electron transfer is shortened, enhancing the anode's electrical conductivity. This mitigates electrical insulation and improves electrode dynamics during cycles. In terms of optical applications, silicon nanoparticles exhibit structural colors due to Mie resonance. Structural colors can also be realized based on the surface plasmon resonance of nanostructures [58]. However, to achieve high color purity over a wide color spectrum, complex structures such as multilayer and asymmetric metal-dielectric nanostructures are required. Silicon nanoparticles offers an angle-insensitive structural color spanning the entire visible spectrum with simple structure, making it a viable candidate for color ink (Fig. 4b) [52]. In order to dye the substrate with a color identical to that of a solution dispersed with silicon nanoparticles, it is necessary to keep the inter-particle distance over 50 nm while solidifying the ink. For this purpose, a methanol solution with dispersed silicon nanoparticles was first mixed with a polyvinylpyrrolidone (PVP) solution to prevent particle aggregation, then the mixture was drop-casted onto the substrate. This allows for painting the substrate with color ink. Furthermore, such Mie resonance, when coupled with a metallic substrate, can realize new resonant modes, enabling the fabrication of nano-antennas [59]. The nano-antenna was fabricated by depositing a monolayer of quantum dots onto the substrate through drop casting, followed by drying in air at room temperature. Finally, a solution with dispersed silicon particles was dropped onto the silicon quantum dot monolayer and dried.

Another energy application involves the fabrication of photovoltaic devices. Ultra-thin silicon solar cells often suffer from low efficiency due to their insufficient thickness for light absorption. By arranging silicon nanoparticles in multilayers, they can be utilized as light-capturing absorbers for ultra-thin solar cells while simultaneously forming a p-n junction (Fig. 4c) [53]. Devices with such a structure can achieve a short circuit current density of up to 26 mA/cm^2, which is promising for monocrystalline silicon ultra-thin solar cells, considering that devices of similar thickness exhibit values below 15 mA/cm^2 [60]. Conversely, silicon nanoparticles can be utilized to fabricate light-emitting diodes (LEDs) (Fig. 4d) [54]. Quantum
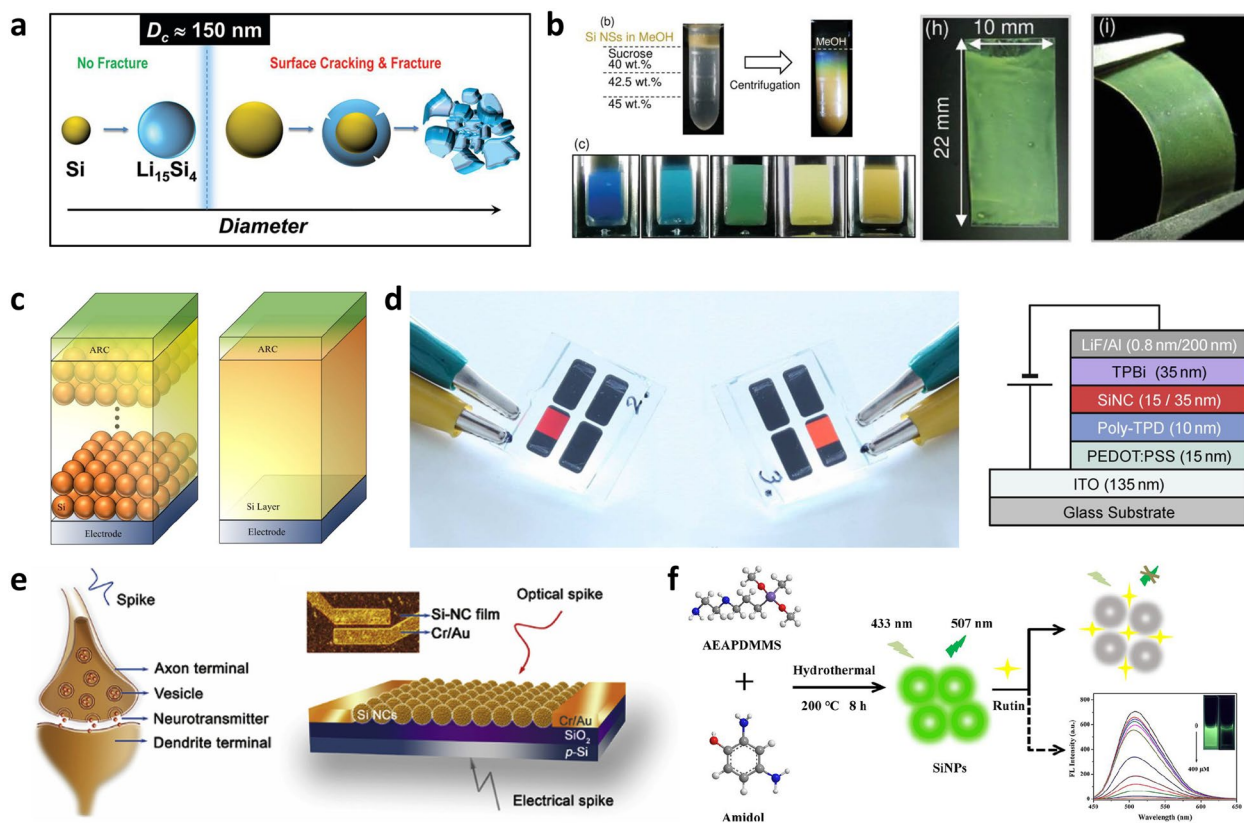
Fig. 4 a Lithiation process of silicon nanoparticles. Cracks do not occur below 150 nm in diameter. Reprinted from [2] with permission from American Chemical Society. **b** (left) Photographs of solutions of size-separated silicon nanoparticles. (right) Silicon nanoparticle-PVP film on PET substrate bent at bending radius of 9 mm. Reprinted from [52] (CC BY 4.0). **c** (left) The schematic of a structure composed of identical silicon nanoparticles and an ARC on the top. (right) A simple planar structure with silicon thickness identical to left. Reprinted from [53] (CC BY 4.0). **d** (left) Photograph of SiLED. (right) Schematic view of SiLED stack. Reprinted from [54] with permission from American Chemical Society. **e** (left) Schematic of a biological synapse. (right) Schematic of a synaptic silicon nanoparticle phototransistor. Reprinted from [55] with permission from Elsevier. **f** Schematic of the synthesis method of the silicon nanoparticles and their use for rutin detection. Reprinted from [56] (CC BY 4.0)

dots made by reducing the size of silicon nanoparticles to below 5 nm can be used to produce LEDs, with tunability ranging from red to yellow-orange spectrum regions. The LED was fabricated by spin-coating various functional layers onto a glass substrate covered with an ITO structure produced through lithography, followed by a thermal evaporation step for the cathode. These LEDs offer the advantage of a high external quantum efficiency and low turn-on voltages.

Similar to fabricating transistors from silicon, silicon nanoparticles can also be utilized to fabricate transistors. Recent advancements have reported the development of synaptic optical transistors, which can be stimulated by optical and electrical spikes utilizing the optical absorption of silicon nanoparticles (Fig. 4e) [55]. For the fabrication of a synaptic device, a solution with dispersed silicon nanoparticles is drop-casted between electrodes spaced at a specific distance apart, and subsequently baked at 150 °C for 30 min to form

a film. These synaptic silicon phototransistors could potentially offer low energy consumption, leading to more efficient devices. Moreover, water-soluble silicon nanopaticles are emerging as compact fluorescent silicon nanomaterials (Fig. 4f) [56]. Compared to conventional fluorescent quantum dots, water-soluble silicon nanoparticles have a simpler composition and are devoid of heavy metal elements. Fluorescent probes can be fabricated by adding a solution dispersed with silicon nanoparticles to PBS solution, mixing evenly, and then adding rutin solutions of various volumes to prepare a series of solutions. Silicon nanoparticles can be metabolized in the body into orthosilicic acid and subsequently excreted through urine, ensuring they're non-toxic. Crucially, due to their outstanding optical properties, robust stability, and excellent biocompatibility, silicon nanoparticles are well-suited as fluorescent probes.

Perspectives

The future of silicon nanoparticles is heavily contingent upon the mass-production capability with high quality and low cost. With advancements in synthesis techniques allowing for large-scale production, consistent quality control remains challenges. In addition, uniformity in particle size, shape, and properties is essential for both fundamental research and commercial applications. It is evident that a production process that enables aforementioned uniformity efficiently will become a gold standard. Moreover, cost reduction is imperative. As research advances and more innovative production techniques become available, the production cost will certainly drop, making it easier to access silicon nanoparticles across various industrial sectors.

The adoption of *in-situ* measurement techniques, where silicon nanoparticles are characterized in real-time during synthesis, provides evidences that were previously unattainable. These techniques provide instant feedback, facilitating adjustments in the production process to obtain desired properties. In addition, the push towards high-speed and high-throughput metrologies ensures that vast quantities of silicon nanoparticles can be characterized quickly, facilitating quality control in mass production scenarios.

Conclusion

In this review, we aim to overview silicon nanoparticle technology. We focuses on fabrication methods of silicon nanoparticles, specifically categorizing top-down, bottom-up and reduction approaches. We also look into various characterization techniques crucial for fabricated silicon nanoparticles. While silicon nanoparticles have been widely utilized in energy and optics applications due to their inherent benefits, there still remains room for further improvement, particularly in fabrication and characterization. Advancements in silicon nanoparticles will undoubtedly pave the way for development of new applications.

Author contributions
TK: Conceptualization, Visualization, Writing, Editing. JL: Supervision, Writing, Editing. Both authors read and approved the final manuscript.

Declarations

Competing interests
JL is the editor-in-chief of Micro and Nano Systems Letters. TK has no competing interests to disclose.

References
1. Casimir A, Zhang H, Ogoke O, Amine JC, Lu J, Wu G (2016) Silicon-based anodes for lithium-ion batteries: effectiveness of materials synthesis and electrode preparation. Nano Energy 27:359–376
2. Liu XH, Zhong L, Huang S, Mao SX, Zhu T, Huang JY (2012) Size-dependent fracture of silicon nanoparticles during lithiation. ACS Nano 6(2):1522–1531
3. Okazaki T, Sugimoto H, Hinamoto T, Fujii M (2021) Color toning of mie resonant silicon nanoparticle color inks. ACS Appl Mater Interfaces 13(11):13613–13619
4. Chaâbani W, Proust J, Movsesyan A, Béal J, Baudrion A-L, Adam P-M, Chehaidar A, Plain J (2019) Large-scale and low-cost fabrication of silicon mie resonators. ACS Nano 13(4):4199–4208
5. Zywietz U, Evlyukhin AB, Reinhardt C, Chichkov BN (2014) Laser printing of silicon nanoparticles with resonant optical electric and magnetic responses. Nat Commun. https://doi.org/10.1038/ncomms4402
6. Maeng S-H, Lee H, Kim S (2021) Synthesis of silicon nanoparticles using a novel reactor with an elongated reaction zone created by coaxially aligned SiH_4 gas and a CO_2 laser beam. J Nanopart Res. https://doi.org/10.1007/s11051-021-05262-w
7. Mangolini L, Thimsen E, Kortshagen U (2005) High-yield plasma synthesis of luminescent silicon nanocrystals. Nano Lett 5(4):655–659
8. Lin N, Han Y, Wang L, Zhou J, Zhou J, Zhu Y, Qian Y (2015) Preparation of nanocrystalline silicon from $SiCl_4$ at 200 °C in molten salt for high-performance anodes for lithium ion batteries. Angew Chem Int Edit 127(12):3893–3896
9. Maeng S-H, Lee H, Park MS, Park S, Jeong J, Kim S (2020) Ultrafast carbothermal reduction of silica to silicon using a CO_2 laser beam. Sci Rep. https://doi.org/10.1038/s41598-020-78562-1
10. Kim KH, Lee DJ, Cho KM, Kim SJ, Park J-K, Jung H-T (2015) Complete magnesiothermic reduction reaction of vertically aligned mesoporous silica channels to form pure silicon nanoparticles. Sci Rep. https://doi.org/10.1038/srep09014
11. Maniya NH, Patel SR, Murthy ZVP (2014) Study on surface chemistry and particle size of porous silicon prepared by electrochemical etching. Mater Res Bull 57:6–12
12. Rodriguez I, Shi L, Lu X, Korgel BA, Alvarez-Puebla RA, Meseguer F (2014) Silicon nanoparticles as raman scattering enhancers. Nanoscale 6(11):5666–5670
13. Krivonosov A, Zuev D, Kaputkina S, Mikhailovskii V, Egorova E, Ageev E, Odintsova G (2020) Evolution of size distribution of Si nanoparticles produced by pulsed laser ablation in water. Opt Quantum Electron. https://doi.org/10.1007/s11082-020-02274-z
14. Intartaglia R, Bagga K, Brandi F (2014) Study on the productivity of silicon nanoparticles by picosecond laser ablation in water: towards gram per hour yield. Opt Express 22(3):3117
15. Kuzmin PG, Shafeev GA, Bukin VV, Garnov SV, Farcau C, Carles R, Warot-Fontrose B, Guieu V, Viau G (2010) Silicon nanoparticles produced by femtosecond laser ablation in ethanol: Size control, structural characterization, and optical properties. J Phys Chem C 114(36):15266–15273
16. Tiberi M, Simonelli A, Cristoforetti G, Marsili P, Giammanco F, Giorgetti E (2012) Effect of picosecond laser induced cavitation bubbles generated on au targets in a nanoparticle production set-up. Appl Phys A Mater Sci Process 110(4):857–861
17. Zywietz U, Reinhardt C, Evlyukhin AB, Birr T, Chichkov BN (2013) Generation and patterning of Si nanoparticles by femtosecond laser pulses. Appl Phys A Mater Sci Process 114(1):45–50
18. Kabashin AV, Singh A, Swihart MT, Zavestovskaya IN, Prasad PN (2019) Laser-processed nanosilicon: a multifunctional nanomaterial for energy and healthcare. ACS Nano 13(9):9841–9867
19. Kim S, Hwang C, Park SY, Ko S-J, Park H, Choi WC, Kim JB, Kim DS, Park S, Kim JY, Song H-K (2014) High-yield synthesis of single-crystal silicon nanoparticles as anode materials of lithium ion batteries via photosensitizer-assisted laser pyrolysis. J Mater Chem A 2(42):18070–18075

20. Huisken F, Ledoux G, Guillois O, Reynaud C (2002) Light-emitting silicon nanocrystals from laser pyrolysis. Adv Mater 14(24):1861–1865
21. Heath JR (1992) A liquid-solution-phase synthesis of crystalline silicon. Science 258(5085):1131–1133
22. Bley RA, Kauzlarich SM (1996) A low-temperature solution phase route for the synthesis of silicon nanoclusters. J Am Chem Soc 118(49):12461–12462
23. Kim H, Seo M, Park M-H, Cho J (2010) A critical size of silicon nano-anodes for lithium rechargeable batteries. Angew Chem Int Edit 122(12):2192–2195
24. Allendorf MD, Melius CF, Ho P, Zachariah MR (1995) Theoretical study of the thermochemistry of molecules in the Si-O-H system. J Phys Chem 99(41):15285–15293
25. Lee H, Lee S, Kim S (2021) Development of silicon nanoparticle production technology using a CO_2 laser-assisted carbothermal reduction process. J Korean Soc Precis Eng 30(4):253–258
26. Martell SA, Lai Y, Traver E, MacInnis J, Richards DD, MacQuarrie S, Dasog M (2019) High surface area mesoporous silicon nanoparticles prepared via two-step magnesiothermic reduction for stoichiometric CO_2 to CH_3OH conversion. ACS Appl Nano Mater 2(9):5713–5719
27. Entwistle J, Rennie A, Patwardhan S (2018) A review of magnesiothermic reduction of silica to porous silicon for lithium-ion battery applications and beyond. J Mater Chem A 6(38):18344–18356
28. Bao Z, Weatherspoon MR, Shian S, Cai Y, Graham PD, Allan SM, Ahmad G, Dickerson MB, Church BC, Kang Z III, HWA, Summers CJ, Liu M, Sandhage KH, (2007) Chemical reduction of three-dimensional silica micro-assemblies into microporous silicon replicas. Nature 446(7132):172–175
29. Hemaprabha E, Pandey UK, Chattopadhyay K, Ramamurthy PC (2018) Doped silicon nanoparticles for enhanced charge transportation in organic-inorganic hybrid solar cells. Sol Energy 173:744–751
30. Scriba MR, Britton DT, Härting M (2011) Electrically active, doped monocrystalline silicon nanoparticles produced by hot wire thermal catalytic pyrolysis. Thin Solid Films 519(14):4491–4494
31. Ge M, Rong J, Fang X, Zhang A, Lu Y, Zhou C (2013) Scalable preparation of porous silicon nanoparticles and their application for lithium-ion battery anodes. Nano Res 6(3):174–181
32. Thiessen AN, Ha M, Hooper RW, Yu H, Oliynyk AO, Veinot JGC, Michaelis VK (2019) Silicon nanoparticles: are they crystalline from the core to the surface? Chem Mat 31(3):678–688
33. Elangovan H, Sengupta S, Narayanan R, Chattopadhyay K (2020) Silicon nanoparticles with UV range photoluminescence synthesized through cryomilling induced phase transformation and etching. J Mater Sci 56(2):1515–1526
34. Doğan İ, van de Sanden MCM (2013) Direct characterization of nanocrystal size distribution using raman spectroscopy. J Appl Phys. https://doi.org/10.1063/1.4824178
35. Zou J, Sanelle P, Pettigrew KA, Kauzlarich SM (2006) Size and spectroscopy of silicon nanoparticles prepared via reduction of SiCl4. J Clust Sci 17(4):565–578
36. Hülser T, Schnurre SM, Wiggers H, Schulz C (2011) Gas-phase synthesis of nanoscale silicon as an economical route towards sustainable energy technology. KONA Powder Part J 29:191–207
37. Wen X, Zhang P, Smith TA, Anthony RJ, Kortshagen UR, Yu P, Feng Y, Shrestha S, Coniber G, Huang S (2015) Tunability limit of photoluminescence in colloidal silicon nanocrystals. Sci Rep. https://doi.org/10.1038/srep12469
38. Lai SY, Knudsen KD, Sejersted BT, Ulvestad A, Mæhlen JP, Koposov AY (2019) Silicon nanoparticle ensembles for lithium-ion batteries elucidated by small-angle neutron scattering. ACS Appl Energ Mater 2(5):3220–3227
39. Wang Q, Bao Y, Zhang X, Coxon PR, Jayasooriya UA, Chao Y (2012) Uptake and toxicity studies of poly-acrylic acid functionalized silicon nanoparticles in cultured mammalian cells. Adv Healthc Mater 1(2):189–198
40. Jain N, Jain P, Rajput D, Patil UK (2021) Green synthesized plant-based silver nanoparticles: therapeutic prospective for anticancer and antiviral activity. Micro Nano Syst Lett. https://doi.org/10.1186/s40486-021-00131-6
41. Minelli C, Sikora A, Garcia-Diez R, Sparnacci K, Gollwitzer C, Krumrey M, Shard AG (2018) Measuring the size and density of nanoparticles by centrifugal sedimentation and flotation. Anal Methods 10(15):1725–1732
42. Ko J, Lee D, Lee BJ, Kauh SK, Lee J (2019) Micropipette resonator enabling targeted aspiration and mass measurement of single particles and cells. ACS Sens 4(12):3275–3282
43. Ko J, Jeong J, Son S, Lee J (2021) Cellular and biomolecular detection based on suspended microchannel resonators. Biomed Eng Lett 11(4):367–382
44. Ulvestad A, Reksten AH, Andersen HF, Carvalho PA, Jensen IJT, Nagell MU, Mæhlen JP, Kirkengen M, Koposov AY (2020) Crystallinity of silicon nanoparticles: direct influence on the electrochemical performance of lithium ion battery anodes. ChemElectroChem 7(21):4349–4353
45. Choi D, Kim JH, Kwon DC, Shin CH, Ryu H, Yoon E, Lee H-C (2021) Crystalline silicon nanoparticle formation by tailored plasma irradiation: self-structurization, nucleation and growth acceleration, and size control. Nanoscale 13(23):10356–10364
46. Tan D, Ma Z, Xu B, Dai Y, Ma G, He M, Jin Z, Qiu J (2011) Surface passivated silicon nanocrystals with stable luminescence synthesized by femtosecond laser ablation in solution. Phys Chem 13(45):20255
47. Fu YH, Kuznetsov AI, Miroshnichenko AE, Yu YF, Luk'yanchuk B (2013) Directional visible light scattering by silicon nanoparticles. Nat Commun. https://doi.org/10.1038/ncomms2538
48. Evlyukhin AB, Novikov SM, Zywietz U, Eriksen RL, Reinhardt C, Bozhevolnyi SI, Chichkov BN (2012) Demonstration of magnetic dipole resonances of dielectric nanospheres in the visible region. Nano Lett 12(7):3749–3755
49. Sharma A, Sagar A, Rana J, Rani R (2022) Green synthesis of silver nanoparticles and its antibacterial activity using fungus talaromyces purpureogenus isolated from taxus baccata linn. Micro Nano Syst Lett. https://doi.org/10.1186/s40486-022-00144-9
50. Priolo F, Gregorkiewicz T, Galli M, Krauss TF (2014) Silicon nanostructures for photonics and photovoltaics. Nat Nanotechnol 9(1):19–32
51. Jurbergs D, Rogojina E, Mangolini L, Kortshagen U (2006) Silicon nanocrystals with ensemble quantum yields exceeding 60%. Appl Phys Lett. https://doi.org/10.1063/1.2210788
52. Sugimoto H, Okazaki T, Fujii M (2020) Mie resonator color inks of mono-dispersed and perfectly spherical crystalline silicon nanoparticles. Adv Opt Mater. https://doi.org/10.1002/adom.202000033
53. Mirnaziry SR, Shameli MA, Yousefi L (2022) Design and analysis of multi-layer silicon nanoparticle solar cells. Sci Rep. https://doi.org/10.1038/s41598-022-17677-z
54. Maier-Flaig F, Rinck J, Stephan M, Bocksrocker T, Bruns M, Kübel C, Powell AK, Ozin GA, Lemmer U (2013) Multicolor silicon light-emitting diodes (SiLEDs). Nano Lett 13(2):475–480
55. Yin L, Han C, Zhang Q, Ni Z, Zhao S, Wang K, Li D, Xu M, Wu H, Pi X, Yang D (2019) Synaptic silicon-nanocrystal phototransistors for neuromorphic computing. Nano Energy 63:103859
56. Pan C, Qin X, Lu M, Ma Q (2022) Water soluble silicon nanoparticles as a fluorescent probe for highly sensitive detection of rutin. ACS Omega 7(32):28588–28596
57. Yang Y, Yuan W, Kang W, Ye Y, Yuan Y, Qiu Z, Wang C, Zhang X, Ke Y, Tang Y (2020) Silicon-nanoparticle-based composites for advanced lithium-ion battery anodes. Nanoscale 12(14):7461–7484
58. Miyata M, Hatada H, Takahara J (2016) Full-color subwavelength printing with gap-plasmonic optical antennas. Nano Lett 16(5):3166–3172
59. Sugimoto H, Fujii M (2018) Broadband dielectric-metal hybrid nanoantenna: silicon nanoparticle on a mirror. ACS Photonics 5(5):1986–1993
60. Massiot I, Cattoni A, Collin S (2020) Progress and prospects for ultrathin solar cells. Nat Energy 5(12):959–972

Publisher's Note